Energy-Efficient Trajectory Planning for a Multi-UAV-Assisted Mobile Edge Computing System[*]

Pei-Qiu Huang[1], Yong Wang[‡1], Kezhi Wang[2]

[1]*School of Automation, Central South University, Changsha 410083, China*
[2]*Department of Computer and Information Sciences, Northumbria University, Newcastle NE1 8ST, U.K.*
E-mail: pqhuang@csu.edu.cn; ywang@csu.edu.cn; kezhi.wang@northumbria.ac.uk

Abstract: This paper studies a mobile edge computing system assisted by multiple unmanned aerial vehicles (UAVs), where the UAVs act as edge servers to provide computing services for Internet of Things devices. Our goal is to minimize the energy consumption of this system by planning the trajectories of these UAVs. This problem is difficult to address because when planning the trajectories, we need to not only consider the order of stop points (SPs), but also their deployment (including the number and location) and the association between UAVs and SPs. To tackle this problem, we present an energy-efficient trajectory planning algorithm (called TPA), which comprises three phases. In the first phase, a differential evolution algorithm with a variable population size is adopted to update the number and locations of SPs at the same time. Then, the second phase employs the k-means clustering algorithm to group the given SPs into a set of clusters, where the number of clusters is equal to that of UAVs and each cluster contains all SPs visited by the same UAV. Finally, in the third phase, to quickly generate the trajectories of UAVs, we propose a low-complexity greedy method to construct the order of SPs in each cluster. Compared with other algorithms, the effectiveness of TPA is verified on a set of instances at different scales.

Key words: multi-unmanned aerial vehicle; mobile edge computing; trajectory planning; differential evolution; k-means clustering algorithm; greedy method

https://doi.org/10.1631/FITEE.1000000   **CLC number:** TP27

1 Introduction

With the development of mobile communication technology and the popularization of Internet of Things (IoT) devices, a considerable number of resource-intensive applications are emerging, such as face recognition, virtual reality, and online games (Zhang et al., 2019; Xu et al., 2018). Despite the growing capabilities of IoT devices, their computing and battery capacities remain insufficient due to

physical size limitations. Therefore, it is a challenge to execute resource-intensive tasks on IoT devices.

Mobile edge computing (MEC) is recognized as a promising technology to address the above challenge. It provides computing services to IoT devices by offloading tasks to edge servers at the edge of the network (Huang et al., 2019; Wang et al., 2019a; Jin et al., 2019). In this way, MEC can reduce latency and energy consumption during task execution. However, MEC still has some limitations. For example, the locations of edge servers are usually fixed and cannot be adjusted according to user requirements. In addition, in large-scale natural disasters, the existing terrestrial communication networks could be destroyed, in which case, it would be difficult for MEC to provide timely services (Mozaffari

---

ⓘ ORCID: Yong Wang, https://orcid.org/0000-0001-7670-3958

et al., 2019).

Unmanned aerial vehicles (UAVs), due to their autonomy and flexibility, have been widely used in various fields (Low et al., 2019; Zaini and Xie, 2020; Zollars et al., 2019). Recently, some attempts have been made to use UAVs to enhance the capabilities of MEC systems. Zhang et al. (2018) explored the energy-aware dynamic resource allocation problem for a UAV-assisted MEC system over Internet of Vehicles. Du et al. (2019) optimized joint resource and workflow scheduling in a UAV-enabled wirelessly powered MEC system. Garg et al. (2018) investigated the application of a UAV-empowered MEC system in cyber-threat detection of smart vehicles. In addition, in order to take full advantage of the high mobility of a UAV, some researchers have focused on trajectory planning in UAV-assisted MEC systems. For instance, Diao et al. (2019) optimized joint trajectory and data allocation to minimize the maximum energy consumption. Jeong et al. (2018) studied the bit allocation and trajectory planning under latency and energy budget constraints. Hu et al. (2019) developed a UAV-assisted relaying and MEC system, where the UAV can act as the MEC server or the relay. Then, the authors proposed a joint task scheduling and trajectory optimization algorithm to minimize the weighted sum energy consumption of the system.

However, the above-mentioned studies only considered single-UAV-assisted MEC systems. In fact, collaboration among multiple UAVs can improve the capability of such systems (Chen et al., 2016). Therefore, some papers have studied multi-UAV-assisted MEC systems, where a group of UAVs, rather than a single UAV, act as edge servers to provide computing services for IoT devices (Zhang et al., 2020; Li et al., 2020). For example, Yang et al. (2019) optimized the power consumption of a multi-UAV-assisted MEC system by considering the joint device association, power control, computing capacity allocation, and location planning. Wang et al. (2020) designed a two-layer optimization algorithm for joint UAV deployment and task scheduling in a multi-UAV-assisted MEC system. Chen et al. (2019) investigated the quality of service in a multi-UAV-assisted MEC system.

In this paper, we investigate the trajectory planning problem in a multi-UAV-assisted MEC system. Compared with conventional trajectory plan-

ning problems (e.g., traveling salesman problems (Huang et al., 2017) and vehicle routing problems (Wang et al., 2016)), the studied problem is more challenging due to the fact that the deployment of the stop points (SPs) of UAVs is unknown *a priori*. In addition, different from trajectory planning problems in single-UAV-assisted MEC systems, in the case of multiple UAVs, we need to consider the association between UAVs and SPs. That is, for a given SP, we need to assign a specific UAV to visit it. The main contributions of this paper are summarized as follows:

- A trajectory planning problem in a multi-UAV-assisted MEC system is formulated with the aim of minimizing the energy consumption of the system by considering the deployment (including the number and locations) of SPs, the association between UAVs and SPs, and the order of SPs.

- An energy-efficient trajectory planning algorithm, called TPA, is proposed to tackle the trajectory planning problem. TPA consists of three phases. First, a differential evolution (DE) algorithm with a variable population is adopted to optimize the deployment of SPs. Subsequently, the k-means clustering algorithm is used to group the given SPs into several clusters, SPs in each of which are associated with the same UAV to be visited. Finally, a greedy method is proposed to construct the order of SPs in each cluster.

- Extensive experiments are carried out on a set of instances with up to 200 IoT devices. The experimental results demonstrate that TPA achieves a better performance compared with other algorithms.

The rest of this paper is organized as follows. In Section 2, the system model and problem formulation are introduced. Section 3 describes the details of the proposed algorithm. The experimental studies are given in Section 4. Finally, Section 5 concludes this paper.
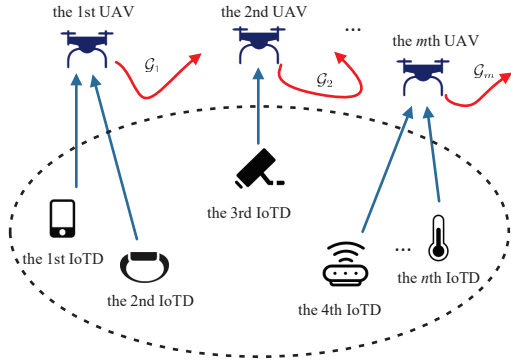
Fig. 1 A multi-UAV-assisted MEC system involving m rotary-wing UAVs and n IoT devices

2 System model and problem formulation

As shown in Figure 1, we consider a multi-UAV-assisted MEC system involving n IoT devices (denoted as $\mathcal{N} = \{1, 2, \cdots, n\}$) and m rotary-wing UAVs with edge servers (denoted as $\mathcal{M} = \{1, 2, \cdots, m\}$). In this system, each IoT device has a resource-intensive task to be completed. For the sake of simplicity, the ith task[1] is expressed as a 2-tuple: (D_i, S_i), where D_i and S_i denote the size of the input data of the ith task and the computing resources required to complete a single bit in the ith task, respectively. Due to the limited computing capacity, these tasks are first offloaded to the MEC servers, and then their results are returned to the IoT devices after the computation is complete.

In this paper, the UAVs can change their SPs to reduce the distance from the IoT devices. We define the set of SPs of the jth UAV as $\mathcal{K}_j = \{1, 2, \cdots, k_j\}$, where k_j is the number of SPs of the jth UAV and it is unknown *a priori*. Moreover, the trajectory of the jth UAV is represented as a sequence of SPs in $\mathcal{K}_j$: $\mathcal{G}_j = \{(X_{j1}, Y_{j1}), (X_{j2}, Y_{j2}), \cdots, (X_{jk_j}, Y_{jk_j})\}$, where $(X_{jl}, Y_{jl}), l \in \mathcal{K}_j$, denotes the location of the lth SP of the jth UAV. Note that, like (Wang et al., 2020) and (Huang et al., 2020), we assume that the UAVs fly at a fixed altitude H, therefore we only show the values on the x-axis and y-axis. In addition, all SPs in $\mathcal{G}_j$ are visited by the jth UAV one by one, where the first SP is visited first and the k_j-th SP is visited last.

We assume that the ith IoT device is located at $(x_i, y_i, 0)$. Therefore, the distance between the ith IoT device and the jth UAV at the lth SP is expressed as

$$d_{ijl} = \sqrt{(x_i - X_{jl})^2 + (y_i - Y_{jl})^2 + H^2},$$
$$\forall i \in \mathcal{N}, j \in \mathcal{M}, l \in \mathcal{K}_j. \quad (1)$$

In order to reduce the transmission time and energy consumption, IoT devices always send their tasks to the closest SP. We define variable a_{ijl} to represent the association between the ith IoT device and the jth UAV at the lth SP. Specifically, $a_{ijl} = 1$ if the ith IoT device is served by the jth UAV at the lth SP; otherwise, $a_{ijl} = 0$. Thus, one can obtain

$$\mathcal{C}1 : a_{ijl} = \begin{cases} 1, & \text{if } (j, l) = \underset{j \in \mathcal{M}, l \in \mathcal{K}_j}{\arg\min} \, d_{ijl}, \\ 0, & \text{otherwise.} \end{cases} \quad (2)$$

Since each task cannot be further divided into subtasks, the following constraint should be satisfied:

$$\mathcal{C}2 : \sum_{j=1}^{m} \sum_{l=1}^{k_j} a_{ijl} = 1, \; \forall i \in \mathcal{N}. \quad (3)$$

Due to the bandwidth limitation, the jth UAV at the lth SP can simultaneously serve at most M IoT devices. Thus, one has

$$\mathcal{C}3 : \sum_{i=1}^{n} a_{ijl} \leq M, \; \forall j \in \mathcal{M}, l \in \mathcal{K}_j. \quad (4)$$

Moreover, each UAV at each SP serves at least one IoT device, thus the total number of SPs of all UAVs, denoted as k, should satisfy the following constraint:

$$\mathcal{C}4 : \; k_{min} \leq k \leq k_{max} \quad (5)$$

where $k = \sum_{j=1}^{m} k_j$; k_{min} and k_{max} are equal to $\lfloor \frac{n}{M} \rfloor$ and n, respectively; and $\lfloor \cdot \rfloor$ denotes the rounding down operator.

The transmission rate of the ith IoT device for sending data to the jth UAV at the lth SP is expressed as

$$r_{ijl} = B \log_2 \left(1 + \frac{p_i^t h_0}{\sigma^2 d_{ijl}^2} \right),$$
$$\forall i \in \mathcal{N}, j \in \mathcal{M}, l \in \mathcal{K}_j \quad (6)$$

where p_i^t denotes the transmitting power of the ith IoT device, h_0 denotes the channel power gain at the

---

[1]For the sake of simplicity, in this paper, we refer to the task of the ith IoT device as the ith task.

reference distance $d_0 = 1$ m, σ^2 denotes the white Gaussian noise power, and B denotes the system bandwidth.

The transmission time and energy consumption of the ith IoT device for sending data to the jth UAV at the lth SP are given by

$$T_{ijl}^t = \frac{D_i}{r_{ijl}}, \ \forall i \in \mathcal{N}, j \in \mathcal{M}, l \in \mathcal{K}_j \qquad (7)$$

and

$$E_{ijl}^t = p_i^t T_{ijl}^t = \frac{p_i^t D_i}{r_{ijl}}, \ \forall i \in \mathcal{N}, j \in \mathcal{M}, l \in \mathcal{K}_j. \quad (8)$$

The whole energy consumption of all IoT devices is expressed as[2]

$$E_{iot} = \sum_{i=1}^n \sum_{j=1}^m \sum_{l=1}^{k_j} a_{ijl} E_{ijl}^t. \qquad (9)$$

After receiving the input data, the UAVs start to execute the tasks. Given the computing resources c_{ijl}, the computing time of the ith task on the jth UAV at the lth SP can be obtained by

$$T_{ijl}^c = \frac{D_i S_i}{c_{ijl}}, \ \forall i \in \mathcal{N}, j \in \mathcal{M}, l \in \mathcal{K}_j. \qquad (10)$$

In fact, the jth UAV will not move to the next SP until all tasks sent to the lth SP have been completed. Therefore, the hovering time of the jth UAV at the lth SP is equal to the maximum execution time of all tasks (i.e., the sum of the transmission and computing time), which is given by

$$T_{jl}^h = \max_{i \in \mathcal{N}} \{ a_{ijl}(T_{ijl}^t + T_{ijl}^c) \}, \ \forall j \in \mathcal{M}, l \in \mathcal{K}_j. \ (11)$$

Then, the hovering energy consumption of the jth UAV is given by

$$E_j^h = \sum_{l=1}^{k_j} p^h T_{jl}^h, \forall j \in \mathcal{M}, \qquad (12)$$

where p^h is the hovering power of the UAV.

Furthermore, given the trajectory of the jth UAV (i.e., $\mathcal{G}_j$), the flight time and energy consumption are expressed as

$$T_j^f = \frac{\sum_{l=2}^{k_j} \sqrt{(X_{jl} - X_{j,l-1})^2 + (Y_{jl} - Y_{j,l-1})^2}}{v},$$
$$\forall j \in \mathcal{M} \qquad (13)$$

and

$$E_j^f = p^f T_j^f, \forall j \in \mathcal{M} \qquad (14)$$

where v is the flight speed of the UAV and p^f is the flight power of the UAV.

The whole energy consumption of all UAVs consists of the hovering and flight energy consumption[3], which can be expressed as

$$E_{uav} = \sum_{j=1}^m \left(E_j^h + E_j^f \right). \qquad (15)$$

In this paper, we aim to optimize the trajectories of UAVs (i.e., $\mathcal{G}_1, \mathcal{G}_2, \cdots, \mathcal{G}_m$) to minimize the energy consumption of the system consisting of UAVs and IoT devices. Thus, the problem can be formulated as

$$\min_{\mathcal{G}_1, \mathcal{G}_2, \cdots, \mathcal{G}_m} E_{uav} + \alpha E_{iot}$$
$$\text{s.t.} \quad \mathcal{C}1: a_{ijl} \in \{0, 1\}, \ \forall i \in \mathcal{N}, j \in \mathcal{M}, l \in \mathcal{K}_j$$
$$\mathcal{C}2: \sum_{j=1}^m \sum_{l=1}^{k_j} a_{ijl} = 1, \ \forall i \in \mathcal{N}$$
$$\mathcal{C}3: \sum_{i=1}^n a_{ijl} \leq M, \ \forall j \in \mathcal{M}, l \in \mathcal{K}_j$$
$$\mathcal{C}4: k_{min} \leq k \leq k_{max}$$
$$\mathcal{C}5: X_{min} \leq X_{jl} \leq X_{max}, \ \forall j \in \mathcal{M}, l \in \mathcal{K}_j$$
$$\mathcal{C}6: Y_{min} \leq Y_{jl} \leq Y_{max}, \ \forall j \in \mathcal{M}, l \in \mathcal{K}_j$$
$$(16)$$

where $\alpha \geq 0$ is the weight parameter between the energy consumption of UAVs and IoT devices; X_{min} and X_{max} are the lower and upper bounds of X_{jl}, respectively; and Y_{min} and Y_{max} are the lower and upper bounds of Y_{jl}, respectively.

3 Proposed approach

By analyzing the problem in (16), there are two challenges that need to be considered:

- In order to address the problem in (16), we need to know how many SPs are suitable and where they are located, which UAV is assigned to visit the given SP, and how to visit SPs in turn for each UAV. Therefore, the above problem can be decomposed into three sub-problems:

---

[2]Due to the fact that the size of the output results is smaller than that of the input data of the task, we omit the transmission time and energy consumption of the output results.

[3]Compared with the hovering and flight energy consumption of UAVs, the computing energy consumption of the UAVs is smaller (Wang et al., 2019b); thus, we omit the computing energy consumption of UAVs
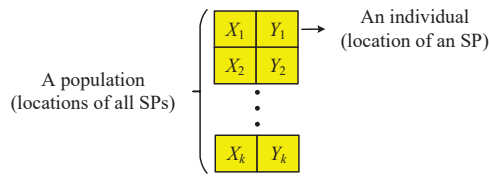
Fig. 2 Encoding mechanism used in this paper

the deployment (including the number and locations) of SPs, the association between UAVs and SPs, and the order of SPs. However, the deployment of SPs, the association between UAVs and SPs, and the order of SPs are coupled with each other. Specifically, the association between UAVs and SPs can be determined only after the deployment of SPs is obtained. Moreover, the order of SPs can be constructed only after the association between UAVs and SPs is determined. Therefore, if they are optimized at the same time, it may lead to poor performance.

- Since the number of SPs is unknown when optimizing their deployment, the gradient information is not available. As a result, traditional gradient-based methods cannot optimize the deployment of SPs. As a class of gradient-free optimization methods, evolutionary algorithms (EAs) have potential for optimizing the deployment of SPs (Zhang et al., 2019). However, in EAs, each individual typically represents an entire deployment. Due to the fact that the number of SPs is unknown *a priori*, the length of the individual is not fixed. However, the commonly used crossover and mutation operators are designed for fixed-length individuals (Ryerkerk et al., 2019). Therefore, using conventional EAs directly would be ineffective in optiming the deployment of SPs.

To this end, we propose a trajectory planning algorithm, called TPA, which has the following technical advantages:

- Considering the strong coupling among the deployment of SPs, the association between UAVs and SPs, and the order of SPs, TPA plans the trajectories of UAVs at each iteration through three phases: update of the deployment of SPs, generation of the association between UAVs and SPs, and construction of the order of SPs.

Algorithm 1 Framework of TPA

1: $FEs = 0$;
2: **repeat**
3:      Produce randomly an initial population $\mathcal{P}$;
4:      Determine the association between UAVs and SPs in $\mathcal{P}$ via the k-means clustering algorithm in **Algorithm 3**;
5:      Construct the order of SPs of each UAV via the greedy method in **Algorithm 4**;
6:      Evaluate $\mathcal{P}$ via (16);
7:      $FEs = FEs + 1$;
8: **until** $\mathcal{P}$ is feasible or $FEs > MaxFEs$
9: **while** $FEs < MaxFEs$ **do**
10:     Produce an offspring population $\mathcal{Q}$ via "DE/rand/1" and the binomial operator of DE;
11:     **for** $i = 1 : |\mathcal{Q}|$ **do**
12:         Construct three new populations $\mathcal{P}_1$, $\mathcal{P}_2$, and $\mathcal{P}_3$ via **Algorithm 2**;
13:         **for** $l = 1 : 3$ **do**
14:             Determine the association between SPs in $\mathcal{P}_l$ and UAVs via the k-means clustering algorithm in **Algorithm 3**;
15:             Construct the order of SPs of each UAV via the greedy method in **Algorithm 4**;
16:         **end for**
17:         Evaluate $\mathcal{P}_1$, $\mathcal{P}_2$, and $\mathcal{P}_3$ via (16);
18:         $FEs = FEs + 3$;
19:         **if** at least one feasible population exists among $\mathcal{P}_1$, $\mathcal{P}_2$, and $\mathcal{P}_3$ **then**
20:             Update $\mathcal{P}$ by the feasible population among $\mathcal{P}_1$, $\mathcal{P}_2$, and $\mathcal{P}_3$ with the greatest performance improvement against $\mathcal{P}$;
21:         **end if**
22:     **end for**
23: **end while**

- As shown in Fig 2, in TPA, each individual represents the location of an SP; thus, the population represents a whole deployment, rather than a set of deployments. Since the length of individuals is the same (i.e., two), we can directly adopt the commonly used crossover and mutation operators for updating the deployment of SPs.

The framework of TPA is presented in **Algorithm 1**. In the initialization, the locations of SPs of all UAVs are produced randomly, forming an initial population $\mathcal{P} = \{(X_1, Y_1), (X_2, Y_2), \cdots, (X_{k_{max}}, Y_{k_{max}})\}$ (line 3). Subsequently, the association between UAVs and SPs in $\mathcal{P}$ is determined using the k-means clustering algo-
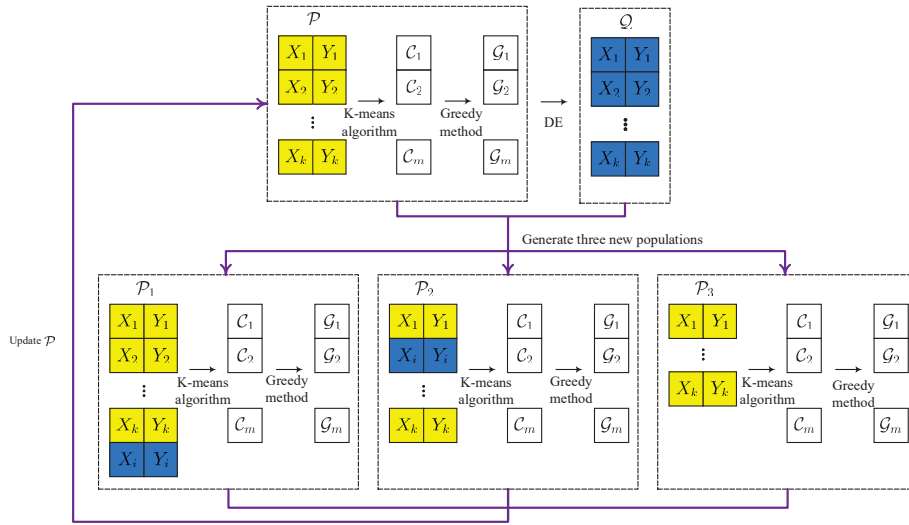
Fig. 3 Overall framework of TPA

Algorithm 2 Generation of three new populations

1: $\mathcal{P}_1 \leftarrow$ insert the ith individual in $\mathcal{Q}$ to $\mathcal{P}$;
2: $\mathcal{P}_2 \leftarrow$ replace a random individual in $\mathcal{P}$ by using the ith individual in $\mathcal{Q}$;
3: $\mathcal{P}_3 \leftarrow$ delete a random individual in $\mathcal{P}$.

---

rithm in **Algorithm** 3 (line 4), and the order of SPs for each UAV is constructed using the greedy method in **Algorithm** 4 (line 5). After that, $\mathcal{P}$ is evaluated via (16) (line 6). If $\mathcal{P}$ is feasible, it is produced successfully; otherwise, the initialization is repeated until $\mathcal{P}$ is feasible or the number of fitness evaluations (FEs) is not less than $MaxFEs$, where $MaxFEs$ denotes the maximum number of FEs. During the evolution, an offspring population $\mathcal{Q}$ is first produced via "DE/rand/1" and the binomial operator of DE (line 10). Subsequently, three new populations $\mathcal{P}_1$, $\mathcal{P}_2$, and $\mathcal{P}_3$ are constructed via **Algorithm** 2 (line 12). Then, the SPs in $\mathcal{P}_1$, $\mathcal{P}_2$, and $\mathcal{P}_3$ are associated with the UAVs via the k-means clustering algorithm in **Algorithm** 3 (line 14), and the order of SPs for each UAV is constructed via the greedy algorithm in **Algorithm** 4 (line 15). Afterward, we evaluate $\mathcal{P}_1$, $\mathcal{P}_2$, and $\mathcal{P}_3$ via (16) (line 17). Finally, the feasible population among $\mathcal{P}_1$, $\mathcal{P}_2$, and $\mathcal{P}_3$ with the greatest performance improvement against $\mathcal{P}$ is used to replace $\mathcal{P}$ if at least one feasible population exists among $\mathcal{P}_1$, $\mathcal{P}_2$, and $\mathcal{P}_3$ (lines $19-21$). The evolution continues until $FEs \geq MaxFEs$. Figure 3 illustrates the overall framework of TPA.

3.1 Update of the deployment of SPs

Updating the deployment of SPs consists of two parts: the locations of SPs and the number of SPs. In TPA, DE (Storn and Price, 1997) is used to update the locations of SPs. The reason is that DE is a simple and effective EA and has been successfully applied in many fields (Wang et al., 2018; Xin et al., 2012). Specifically, we first use "DE/rand/1" and the binomial operator (Wang et al., 2011) of DE to produce an offspring population $\mathcal{Q}$ consisting of the locations of new SPs, and then adopt the individuals in $\mathcal{Q}$ to update $\mathcal{P}$. In this way, the locations of SPs can be updated.

Since the location of each SP is treated as an individual in DE, the whole population represents the locations of all SPs. Therefore, the population size is equal to the number of SPs. In order to update the number of SPs, the population size should be variable during the evolution. In other words, the population size can be increased, kept unchanged, or reduced. As a result, we first construct three populations of different sizes via Algorithm 2. Specifically, for the ith individual in $\mathcal{Q}$, a new population $\mathcal{P}_1$ is constructed by incorporating it into $\mathcal{P}$ and another new population $\mathcal{P}_2$ is constructed by using it to replace a random individual in $\mathcal{P}$. In addition, the third new population $\mathcal{P}_3$ is constructed by removing a random individual from $\mathcal{P}$. It is clear that the population sizes of $\mathcal{P}_1$, $\mathcal{P}_2$, and $\mathcal{P}_3$ are one more

Algorithm 3 K-means clustering algorithm for the clustering of SPs

---

1: Initial $\mathcal{C}_j = \emptyset, \forall j \in \mathcal{M}$;
2: Select randomly an SP for each cluster;
3: **repeat**
4:    **for** $i = 1 : k$ **do**
5:       **for** $j = 1 : m$ **do**
6:          Calculate distance d_{ij} from the ith SP to the center of all SPs in the jth cluster;
7:       **end for**
8:       $j' = \arg\min_{j \in \mathcal{M}} d_{ij}$;
9:       Add the ith SP into $\mathcal{C}_{j'}$;
10:    **end for**
11: **until** The center of SPs in each cluster has no longer changed
12: Associate the jth UAV with SPs in $\mathcal{C}_j, \forall j \in \mathcal{M}$.

---

than, the same as, and one less than that of $\mathcal{P}$, respectively. Therefore, when $\mathcal{P}_1$, $\mathcal{P}_2$, or $\mathcal{P}_3$ is selected to updated $\mathcal{P}$, the population size will be increased, kept unchanged, and reduced, respectively. In this way, the number of SPs can be updated.

3.2 Generation of the association between UAVs and SPs

After generating a new population, we need to determine the association between UAVs and SPs. That is, these SPs are assigned to UAVs to be visited. In this paper, the k-means clustering algorithm (Jain, 2010) is used to group SPs into m clusters, where SPs in each cluster are visited by the same UAV. The loss function of the k-means clustering algorithm in this paper is given as

$$\min_{\mathcal{C}_j, j \in \mathcal{M}} \sum_{j \in \mathcal{M}} \sum_{(X_l, Y_l) \in \mathcal{C}_j} \sqrt{(X_l - \hat{X}_j)^2 + (Y_l - \hat{Y}_j)^2} \tag{17}$$

where $\hat{X}_j = \frac{1}{|\mathcal{C}_j|} \sum_{(X_l, Y_l) \in \mathcal{C}_j} X_l$ and $\hat{Y}_j = \frac{1}{|\mathcal{C}_j|} \sum_{(X_l, Y_l) \in \mathcal{C}_j} Y_l$.

From Eq. (17), we can find that the k-means clustering algorithm can group the closely spaced SPs into the same cluster. Since the SPs in the same cluster are visited by the same UAV, the flying distance of UAVs can be reduced, thereby contributing to savings in energy consumption in the system.

Algorithm 3 presents the procedure for the k-means clustering algorithm for the association between UAVs and SPs. First, we initialize m clusters $\mathcal{C}_j = \emptyset, \forall j \in \mathcal{M}$, and then randomly select an SP for each cluster (lines $1-2$). Afterward, we calculate the

Algorithm 4 Greedy method for constructing the order of SPs

1: **for** $j = 1 : m$ **do**
2:    Select the location of a random SP from $\mathcal{C}_j$ as the current SP of the jth UAV;
3:    **for** $l = 1 : k_j$ **do**
4:       Move the current SP from $\mathcal{C}_j$ into $\mathcal{G}_j$;
5:       Calculate distances from the current SP to all SPs in $\mathcal{C}_j$;
6:       Find the closest SP from the current SP as the new current SP;
7:    **end for**
8: **end for**
9: Output $\mathcal{G}_j, j \in \mathcal{M}$.

---

distance from each SP to the center of SPs in each cluster and add the SP into the nearest cluster (lines 4-10). The above procedure is repeated until the center of SPs in each cluster has no longer changed. Finally, all SPs in $\mathcal{C}_j, \forall j \in \mathcal{M}$, are associated with the jth UAV.

**3.3 Construction of the order of SPs**

In this subsection, we construct the order of SPs for each UAV to minimize the flying distance of UAVs. In fact, this problem is essentially a traveling salesman problem. Although classical mathematical programming methods, such as the branch and bound algorithm, and the population-based methods, such as ant colony algorithm and genetic algorithm (GA), have been successfully adopted to address traveling salesman problems, they suffer from high computational time complexity. To this end, we propose a low-complexity greedy method for constructing the order of SPs.

As shown in **Algorithm 4**, for the first UAV, we first select a random SP from $\mathcal{C}_1$ as the current SP (line 2). Subsequently, the current SP is moved from $\mathcal{C}_1$ into $\mathcal{G}_1$ (line 4). The distances from the current SP to all SPs in $\mathcal{C}_1$ are then calculated and the closest SP from the current SP is chosen as the new current SP (lines 5-6). The above procedure is repeated until $\mathcal{C}_1$ is empty. As a result, the trajectory of the first UAV (i.e., $\mathcal{G}_1$) is generated. The remaining UAVs experience the above process one by one.

Remark: In the existing studies on trajectory planning problems in multi-UAV-assisted MEC systems (Zhang et al., 2020; Li et al., 2020), it is assumed that all UAVs have the same working time. In addition, the working time is divided into a series

Table 1 Experimental results of TPA-VLGA, TPA-JGGA, TPA-DEEM, and TPA in terms of average EC(J) over 20 runs

n	TPA-VLGA Mean(Std Dev)	TPA-JGGA Mean(Std Dev)	TPA-DEEM Feasibility Rate	TPA Mean(Std Dev)
60	$1.57e+6(2.33e+4)\uparrow$	$1.53e+6(2.47e+4)\uparrow$	$90\%\uparrow$	$1.40e+6(2.03e+4)$
80	$2.36e+6(4.20e+4)\uparrow$	$2.22e+6(2.33e+4)\uparrow$	$95\%\uparrow$	$2.06e+6(2.68e+4)$
100	$3.07e+6(3.41e+4)\uparrow$	$2.94e+6(2.79e+4)\uparrow$	$90\%\uparrow$	$2.68e+6(3.73e+4)$
120	$3.28e+6(3.54e+4)\uparrow$	$3.12e+6(2.74e+4)\uparrow$	$80\%\uparrow$	$2.82e+6(6.29e+4)$
140	$4.31e+6(4.39e+4)\uparrow$	$4.09e+6(3.59e+4)\uparrow$	$70\%\uparrow$	$3.71e+6(3.03e+4)$
160	$5.03e+6(6.89e+4)\uparrow$	$4.77e+6(2.59e+4)\uparrow$	$75\%\uparrow$	$4.21e+6(5.21e+4)$
180	$5.63e+6(6.06e+4)\uparrow$	$5.39e+6(3.87e+4)\uparrow$	$85\%\uparrow$	$4.83e+6(4.17e+4)$
200	$6.27e+6(1.00e+5)\uparrow$	$6.07e+6(3.86e+4)\uparrow$	$80\%\uparrow$	$5.35e+6(4.20e+4)$
$\uparrow/\downarrow/\approx$	7/0/0	7/0/0	7/0/0	

(a) $n=160$ (b) $n=180$ (c) $n=200$
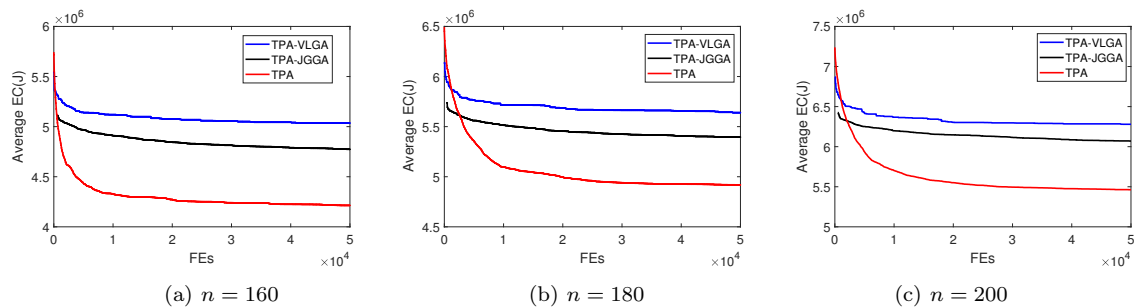
Fig. 4 Evolution of the average EC(J) values obtained by TPA-VLGA, TPA-JGGA, and TPA on three instances.

of time slots in a discretized manner and then the SP of each UAV is determined for each time slot. In this case, all UAVs have the same number of SPs. However, this paper does not assume that all UAVs have the same working time and the same number of SPs.

4 Experimental study

The parameter settings of the studied multi-UAV-assisted MEC system are summarized as follows. We assume that the IoT devices were distributed randomly in a 1000 m∗1000 m square region. There were four UAVs flying at a height of 200 m at a speed of 20 m/s; D_i ($i \in \mathcal{N}$) was distributed randomly in $[1,10^3]$ MB, S_i ($i \in \mathcal{N}$) was set to 100 cycle/bit, c_{ijl} ($i \in \mathcal{N}, j \in \mathcal{M}, l \in \mathcal{K}_j$) was set to 10 Gcycles, M was set to 5, p_i^t was set to 0.1 W, and both p^h and p^f were set to 1000 W. In addition, σ^2 was set to -174 dBm, h_o was set to -30 dB, B was set to 1 MHz, and α was set to 10000. In this paper, we adopted eight instances with different numbers of IoT devices to evaluate the performance of TPA: $n = \{60, 80, 100, 120, 140, 160, 180, 200\}$. The parameters of TPA were set as follows: $F = 0.6$,

$CR = 0.5$, and $MaxFEs = 50000$. Each algorithm was executed independently 20 runs for each instance. Moreover, to test the statistical significance between TPA and each competitor, the Wilcoxon's rank-sum test at a 0.05 significance level was conducted. In the experimental results, "↑", "≈", and "↓" represent that TPA performed significantly better than, equivalent to, and worse than its competitor, respectively. We implemented all the experiments in MATLAB and tested them on a personal computer running with an Intel Core i5-7500 CPU @3.40 GHz and 8 GB of RAM.

4.1 Effectiveness of the deployment of SPs

TPA adopts DE with a variable population to update the deployment of SPs. To verify the effectiveness of the deployment of SPs, we replaced DE used in TPA with three other algorithms: VLGA (Ting et al., 2009), JGGA (Chan et al., 2007), and DEEM (Wang et al., 2018), respectively, resulting in three new algorithms: TPA-VLGA, TPA-JGGA, and TPA-DEEM. In VLGA, the uniform and cut-and-splice crossover operators are used to produce variable-length individuals. JGGA employs continuous auxiliary variables ranging from 0 to 1 to control

the expression of the locations of SPs. If the auxiliary variable is greater than 0.5, the corresponding SP is used; otherwise, it is not used. DEEM develops an encoding mechanism similar to that used in this paper, but it needs to set the number of SPs in advance. In this paper, we preset the number of SPs in DEEM to a random value between $[k_{min}, k_{max}]$.

Table 1 presents the experimental results of TPA and three comparators regarding the average and standard deviation of energy consumption (EC) over 20 runs. The statistical test results between TPA and each of the three competitors are summarized at the bottom of Table 1. Note that, if not all IoT devices are served in one run, the run was considered to be infeasible. In this case, we only give the feasibility rate in Table 1. It is clear that TPA-VLGA, TPA-JGGA, and TPA can achieve a 100% feasibility rate on each instance. However, TPA shows better performance than TPA-VLGA and TPA-JGGA on each instance in terms of the average EC. As for DEEM, it cannot achieve a 100% feasibility rate on any instance. In addition, TPA is significantly better than each of the three competitors on all instances. Figure 4 plots the evolution of the average EC of TPA-VLGA, TPA-JGGA, and TPA when $n = 160, 180$, and 200. Since TPA-DEEM cannot achieve a 100% feasibility rate on these instances, the evolution of the average EC of TPA-DEEM is not presented. It can be seen that TPA provides the best performance in all algorithms. Moreover, we present the average running time of TPA-VLGA, TPA-JGGA, and TPA on each instance in Figure 5. Although the difference among the average running time of TPA-VLGA, TPA-JGGA, and TPA is small, it can still be found that TPA-VLGA, TPA-JGGA, and TPA require less running time on 3, 1, and 4 instances, respectively.

The above-mentioned phenomenon is mainly attributed to the following reasons. Due to the different lengths of individuals, TPA-VLGA searches for the optimal deployment of SPs in a variable-dimensional space, which may cause a confused search. Although the individuals in TPA-JGGA are of the same length, the introduction of auxiliary variables leads to an increase in the length of the individuals, thus encountering the curse of dimensionality, especially in large-scale instances. Since the number of SPs needs to be set in advance, TPA-DEEM cannot update the number of SPs during evolution.
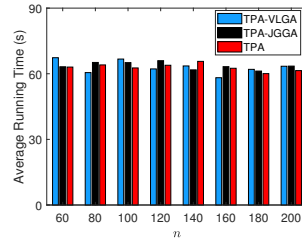

Fig. 5 Average running time of TPA-VLGA, TPA-JGGA, and TPA on each instance.

Note that, an inappropriate number of SPs may result in not all IoT devices being served. Since TPA can simultaneously update the number and location of SPs, and the length of individuals is the same and very low, it can achieve a better performance.

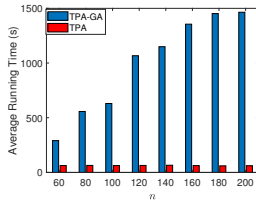### 4.2 Effectiveness of the association between UAVs and SPs

In order to verify the effectiveness of the association between UAVs and SPs, we developed a variant of TPA without the k-means clustering algorithm, called TPA-WoK, in which the UAVs are randomly associated with SPs. Table 2 presents the average and standard deviation of EC over 20 runs, as well as the statistical results between TPA and TPA-WoK. It is clear that TPA outperforms TPA-WoK on all instances in terms of the average EC. In addition, TPA presents significantly better statistical test results on all instances. The reason is given as follows. From Figures 6(a) and 6(b), we can observe that TPA can associate the closely spaced SPs with the same UAV but TPA-WoK cannot. Therefore, TPA can reduce the flight distance of UAVs to lower the energy consumption of the system, which verifies the effectiveness of the association between UAVs and SPs.

4.3 Effectiveness of the order of SPs

In this subsection, we investigated the effectiveness of the order of SPs by comparing TPA with two variants, called TPA-RAN and TPA-GA. TPA-RAN randomly generates the order of SPs, while TPA-GA employs GA to optimize the order of SPs. Note that, in TPA-GA, a population of ten individuals was used to search for the optimal trajectory for each UAV and the maximum number of iterations was set to 50. Table 2 presents the experimental results of TPA-RAN, TPA-GA, and TPA. It is clear

Table 2 Experimental results of TPA-WoK, TPA-RAN, TPA-GA, and TPA in terms of average EC(J) over 20 runs

n	TPA-WoK Mean(Std Dev)	TPA-RAN Mean(Std Dev)	TPA-GA Mean(Std Dev)	TPA Mean(Std Dev)
60	$1.60e+6(5.74e+4)\uparrow$	$1.56e+6(1.97e+5)\uparrow$	$1.43e+6(5.87e+4)\uparrow$	$1.40e+6(2.03e+4)$
80	$2.29e+6(6.89e+4)\uparrow$	$2.48e+6(3.14e+5)\uparrow$	$2.27e+6(3.14e+4)\uparrow$	$2.06e+6(2.68e+4)$
100	$2.99e+6(4.88e+4)\uparrow$	$3.63e+6(4.02e+5)\uparrow$	$3.18e+6(1.72e+5)\uparrow$	$2.68e+6(3.73e+4)$
120	$3.15e+6(5.29e+4)\uparrow$	$4.33e+6(1.71e+5)\uparrow$	$3.71e+6(1.96e+5)\uparrow$	$2.82e+6(6.29e+4)$
140	$4.06e+6(4.88e+4)\uparrow$	$5.51e+6(2.29e+5)\uparrow$	$4.90e+6(1.24e+5)\uparrow$	$3.71e+6(3.03e+4)$
160	$4.66e+6(6.71e+4)\uparrow$	$6.61e+6(1.83e+5)\uparrow$	$5.94e+6(1.05e+5)\uparrow$	$4.21e+6(5.21e+4)$
180	$5.22e+6(6.71e+4)\uparrow$	$7.60e+6(1.45e+5)\uparrow$	$6.69e+6(1.07e+5)\uparrow$	$4.83e+6(4.17e+4)$
200	$5.85e+6(8.88e+4)\uparrow$	$8.51e+6(2.38e+5)\uparrow$	$7.72e+6(2.62e+5)\uparrow$	$5.35e+6(4.20e+4)$
$\uparrow/\downarrow/\approx$	7/0/0	7/0/0	7/0/0	

(a) TPA   (b) TPA-WoK   (c) TPA-RAN   (d) TPA-GA
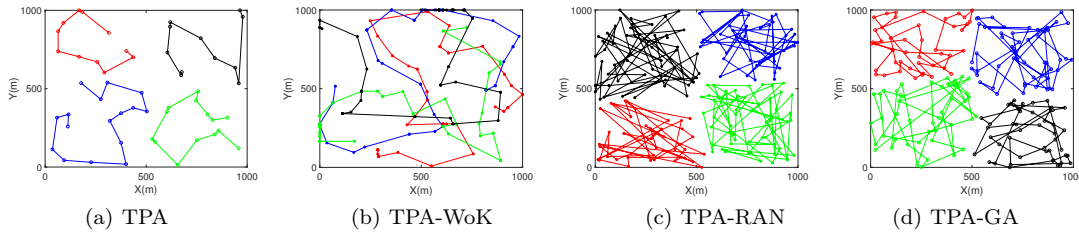
Fig. 6 Trajectories of UAVs obtained by TPA, TPA-WoK, TPA-RAN, and TPA-GA when $n=200$, where the red line, green line, blue line, and black line indicate the trajectories of four UAVs (i.e., $\mathcal{G}_1$, $\mathcal{G}_2$, $\mathcal{G}_3$, and $\mathcal{G}_4$), respectively.

Fig. 7 Average running time of TPA-GA and TPA on each instance.

Table 3 Experimental results of TPA-RPS and TPA in terms of average EC(J) over 20 runs

n	TPA-RPS Mean(Std Dev)	TPA Mean(Std Dev)
60	$1.41e+6(1.73e+4)\approx$	$1.40e+6(2.03e+4)$
80	$2.06e+6(3.19e+4)\approx$	$2.06e+6(2.68e+4)$
100	$2.68e+6(5.29e+4)\approx$	$2.68e+6(3.73e+4)$
120	$2.81e+6(3.17e+4)\approx$	$2.82e+6(6.29e+4)$
140	$3.70e+6(4.06e+4)\approx$	$3.71e+6(3.03e+4)$
160	$4.24e+6(5.27e+4)\approx$	$4.21e+6(5.21e+4)$
180	$4.84e+6(5.37e+4)\approx$	$4.83e+6(4.17e+4)$
200	$5.36e+6(5.59e+4)\approx$	$5.35e+6(4.20e+4)$
$\uparrow/\downarrow/\approx$	0/0/7	

that TPA performs better than TPA-RAN and TPA-GA. To further validate the effectiveness of the order of SPs, we present the trajectories of UAVs obtained by TPA-RAN and TPA-GA in Figures 6(c) and 6(d). Compared with TPA, both TPA-RAN and TPA-GA obtain longer flight trajectories, resulting in higher energy consumption. The above experimental results verify the effectiveness of the order of SPs. The poor performance of TPA-GA could appear confusing. It is explained as follows. As shown in Figure 7, the average running time of TPA-GA is higher than that of TPA due to the fact that GA usually requires more fitness evaluations than the greedy method. As a result, under the given time budget, TPA-GA is likely to perform worse than TPA.

4.4 Discussions

4.4.1 Effect of the Initial Population Size

In this paper, we set the initial population size of TPA to k_{max}. One might be interested in the effect of the initial population size on the performance of TPA. Therefore, in this subsection, the initial population size was set to a random number between $[k_{min}, k_{max}]$. The resulting variant is named TPA-RPS. As shown in Table 3, there is no significant performance difference between TPA and TPA-RPS, which means that the performance of TPA is not sensitive to the initial population size. The reason is that TPA can update the population size adaptively.

Table 4 Experimental results of TPA with Three Different Updating Strategies

n	Five Mean(Std Dev)	Three Mean(Std Dev)	One Mean(Std Dev)
60	$1.52e+6(4.74e+4)\uparrow$	$1.50e+6(3.63e+4)\uparrow$	$1.40e+6(2.03e+4)$
80	$2.22e+6(3.74e+4)\uparrow$	$2.15e+6(4.62e+4)\uparrow$	$2.06e+6(2.68e+4)$
100	$2.84e+6(7.20e+4)\uparrow$	$2.78e+6(5.87e+4)\uparrow$	$2.68e+6(3.73e+4)$
120	$3.01e+6(6.73e+4)\uparrow$	$2.92e+6(7.72e+4)\uparrow$	$2.82e+6(6.29e+4)$
140	$3.95e+6(9.34e+4)\uparrow$	$3.81e+6(7.16e+4)\uparrow$	$3.71e+6(3.03e+4)$
160	$4.44e+6(1.03e+5)\uparrow$	$4.42e+6(8.35e+4)\uparrow$	$4.21e+6(5.21e+4)$
180	$5.08e+6(1.10e+5)\uparrow$	$4.95e+6(1.05e+5)\uparrow$	$4.83e+6(4.17e+4)$
200	$5.75e+6(1.52e+5)\uparrow$	$5.53e+6(1.36e+5)\uparrow$	$5.35e+6(4.20e+4)$
$\uparrow/\downarrow/\approx$	7/0/0	7/0/0	

4.4.2 Effect of the Updating Strategy

In order to investigate the effect of the updating strategy, we tested TPA with three different strategies. Specifically, in each updating, at most one, three, and five individuals in the new population are different from $\mathcal{P}$, respectively. As shown in Table 4, the strategy that can update at most one individual in each updating can provide the best performance among three compared strategies. The above comparison shows that a dramatic change in population size may lead to poor performance. Therefore, TPA updates at most one individual in each updating.

5 Conclusion

In this paper, a multi-UAV-assisted mobile edge computing system was studied. In order to reduce the energy consumption of the system, a trajectory planning problem was formulated, containing three coupled sub-problems: the deployment of SPs, the association between UAVs and SPs, and the order of SPs. To solve the trajectory planning problem, we proposed a three-phase trajectory planning algorithm, called TPA. First, DE with a variable population was used for the deployment of SPs, which can simultaneously update the number and locations of SPs. Subsequently, the k-means clustering algorithm was employed to cluster SPs into a set of subsets with the aim of associating the closely spaced SPs with the same UAV. Moreover, to reduce the flight distances of UAVs, we designed a greedy method that can quickly construct the order of SPs visited by UAVs. The experimental results show that on a set of instances at different scales, TPA can save much energy compared with other algorithms. Therefore, TPA can achieve energy-efficient trajectory planning. However, we need to preset the number of clusters (i.e., the number of UAVs) in the k-means clustering algorithm. As a result, TPA cannot solve the trajectory planning problem for a mobile edge computing system that is assisted by a variable number of UAVs. In the future, we will try to use the clustering algorithm that does not require a preset number of clusters to solve such a trajectory planning problem.

Contributors

Pei-Qiu Huang and Kezhi Wang conceived the idea of the study. Yong Wang refined the idea. Pei-Qiu Huang performed research and wrote the paper. All authors discussed the results and revised the manuscript.

Compliance with ethics guidelines

Pei-Qiu Huang, Yong Wang, and Kezhi Wang declare that they have no conflict of interest.

References

Chan TM, Man KF, Tang KS, et al., 2007. A jumping-genes paradigm for optimizing factory wlan network. *IEEE Transactions on Industrial Informatics*, 3(1):33-43.
https://doi.org/10.1109/TII.2006.890528

Chen J, Zhang X, Xin B, et al., 2016. Coordination between unmanned aerial and ground vehicles: A taxonomy and optimization perspective. *IEEE Transactions on Cybernetics*, 46(4):959-972.
https://doi.org/10.1109/TCYB.2015.2418337

Chen W, Liu B, Huang H, et al., 2019. When UAV swarm meets edge-cloud computing: The QoS perspective. *IEEE Network*, 33(2):36-43.
https://doi.org/10.1109/MNET.2019.1800222

Diao X, Zheng J, Cai Y, et al., 2019. Fair data allocation and trajectory optimization for UAV-assisted mobile edge computing. *IEEE Communications Letters*, 23(12):2357-2361.
https://doi.org/10.1109/LCOMM.2019.2943461

Du Y, Yang K, Wang K, et al., 2019. Joint resources and workflow scheduling in UAV-enabled wirelessly-powered mec for iot systems. *IEEE Transactions on Vehicular Technology*, 68(10):10187-10200.
https://doi.org/10.1109/TVT.2019.2935877

Garg S, Singh A, Batra S, et al., 2018.   UAV-empowered edge computing environment for cyber-threat detection in smart vehicles. *IEEE Network*, 32(3):42-51. https://doi.org/10.1109/MNET.2018.1700286

Hu X, Wong K, Yang K, et al., 2019.   UAV-assisted relaying and edge computing: Scheduling and trajectory optimization. *IEEE Transactions on Wireless Communications*, 18(10):4738-4752. https://doi.org/10.1109/TWC.2019.2928539

Huang L, Wang Gc, Bai T, et al., 2017.   An improved fruit fly optimization algorithm for solving traveling salesman problem. *Frontiers of Information Technology & Electronic Engineering*, 18(10):1525-1533. https://doi.org/10.1631/FITEE.1601364

Huang P, Wang Y, Wang K, et al., 2019. A bilevel optimization approach for joint offloading decision and resource allocation in cooperative mobile edge computing. *IEEE Transactions on Cybernetics*, published online. https://doi.org/10.1109/TCYB.2019.2916728

Huang P, Wang Y, Wang K, et al., 2020. Differential evolution with a variable population size for deployment optimization in a UAV-assisted iot data collection system. *IEEE Transactions on Emerging Topics in Computational Intelligence*, 4(3):324-335. https://doi.org/10.1109/TETCI.2019.2939373

Jain AK, 2010. Data clustering: 50 years beyond k-means. *Pattern Recognition Letters*, 31(8):651 - 666. https://doi.org/10.1016/j.patrec.2009.09.011

Jeong S, Simeone O, Kang J, 2018.   Mobile edge computing via a UAV-mounted cloudlet: Optimization of bit allocation and path planning. *IEEE Transactions on Vehicular Technology*, 67(3):2049-2063. https://doi.org/10.1109/TVT.2017.2706308

Jin Ms, Gao S, Luo Hb, et al., 2019.   Cost-effective resource segmentation in hierarchical mobile edge clouds. *Frontiers of Information Technology & Electronic Engineering*, 20(9):1209-1220. https://doi.org/10.1631/FITEE.1800203

Li M, Cheng N, Gao J, et al., 2020. Energy-efficient UAV-assisted mobile edge computing: Resource allocation and trajectory optimization.   *IEEE Transactions on Vehicular Technology*, 69(3):3424-3438. https://doi.org/10.1109/TVT.2020.2968343

Low JE, Sufiyan D, Win LST, et al., 2019.   Design of a hybrid aerial robot with multi-mode structural efficiency and optimized mid-air transition. *Unmanned Systems*, 07(04):195-213. https://doi.org/10.1142/S2301385019500067

Mozaffari M, Saad W, Bennis M, et al., 2019. A tutorial on UAVs for wireless networks: Applications, challenges, and open problems.   *IEEE Communications Surveys Tutorials*, 21(3):2334-2360. https://doi.org/10.1109/COMST.2019.2902862

Ryerkerk M, Averill R, Deb K, et al., 2019.   A survey of evolutionary algorithms using metameric representations. *Genetic Programming and Evolvable Machines*, 20(4):441-478. https://doi.org/10.1007/s10710-019-09356-2

Storn R, Price K, 1997.   Differential evolution – a simple and efficient heuristic for global optimization over continuous spaces.   *Journal of Global Optimization*, 11(4):341-359. https://doi.org/10.1023/A:1008202821328

Ting C, Lee C, Chang H, et al., 2009.   Wireless heterogeneous transmitter placement using multiobjective variable-length genetic algorithm.   *IEEE Transactions on Systems, Man, and Cybernetics, Part B (Cybernetics)*, 39(4):945-958. https://doi.org/10.1109/TSMCB.2008.2010951

Wang B, Li H, Zhang Q, et al., 2018. Decomposition-based multiobjective optimization for constrained evolutionary optimization. *IEEE Transactions on Systems, Man, and Cybernetics: Systems*, published online. https://doi.org/10.1109/TSMC.2018.2876335

Wang J, Zhou Y, Wang Y, et al., 2016. Multiobjective vehicle routing problems with simultaneous delivery and pickup and time windows: Formulation, instances, and algorithms. *IEEE Transactions on Cybernetics*, 46(3):582-594. https://doi.org/10.1109/TCYB.2015.2409837

Wang K, Huang P, Yang K, et al., 2019a.   Unified offloading decision making and resource allocation in ME-RAN.   *IEEE Transactions on Vehicular Technology*, 68(8):8159-8172. https://doi.org/10.1109/TVT.2019.2926513

Wang L, Huang P, Wang K, et al., 2019b.   RL-based user association and resource allocation for multi-UAV enabled MEC.   2019 15th International Wireless Communications Mobile Computing Conference (IWCMC), p.741-746. https://doi.org/10.1109/IWCMC.2019.8766458

Wang Y, Cai Z, Zhang Q, 2011. Differential evolution with composite trial vector generation strategies and control parameters. *IEEE Transactions on Evolutionary Computation*, 15(1):55-66. https://doi.org/10.1109/TEVC.2010.2087271

Wang Y, Liu H, Long H, et al., 2018. Differential evolution with a new encoding mechanism for optimizing wind farm layout.   *IEEE Transactions on Industrial Informatics*, 14(3):1040-1054. https://doi.org/10.1109/TII.2017.2743761

Wang Y, Ru Z, Wang K, et al., 2020. Joint deployment and task scheduling optimization for large-scale mobile users in multi-UAV-enabled mobile edge computing.   *IEEE Transactions on Cybernetics*, 50(9):3984-3997. https://doi.org/10.1109/TCYB.2019.2935466

Xin B, Chen J, Zhang J, et al., 2012. Hybridizing differential evolution and particle swarm optimization to design powerful optimizers: A review and taxonomy.   *IEEE Transactions on Systems, Man, and Cybernetics, Part C (Applications and Reviews)*, 42(5):744-767. https://doi.org/10.1109/TSMCC.2011.2160941

Xu Jw, Ota K, Dong Mx, et al., 2018. SIoTFog: Byzantine-resilient IoT fog networking. *Frontiers of Information Technology & Electronic Engineering*, 19(12):1546-1557. https://doi.org/10.1631/FITEE.1800519

Yang Z, Pan C, Wang K, et al., 2019. Energy efficient resource allocation in UAV-enabled mobile edge computing networks. *IEEE Transactions on Wireless Communications*, 18(9):4576-4589. https://doi.org/10.1109/TWC.2019.2927313

Zaini AH, Xie L, 2020. Distributed drone traffic coordination using triggered communication.   *Unmanned Systems*, 08(01):1-20. https://doi.org/10.1142/S2301385020500016

Zhang J, Zhou L, Zhou F, et al., 2020. Computation-efficient offloading and trajectory scheduling for multi-UAV assisted mobile edge computing. *IEEE Transactions on Vehicular Technology*, 69(2):2114-2125.
https://doi.org/10.1109/TVT.2019.2960103

Zhang J, Huang T, Wang S, et al., 2019. Future internet: trends and challenges. *Frontiers of Information Technology & Electronic Engineering*, 20(9):1185-1194.
https://doi.org/10.1631/FITEE.1800445

Zhang L, Zhao Z, Wu Q, et al., 2018. Energy-aware dynamic resource allocation in UAV assisted mobile edge computing over social internet of vehicles. *IEEE Access*, 6:56700-56715.
https://doi.org/10.1109/ACCESS.2018.2872753

Zollars MD, Cobb RG, Grymin DJ, 2019. Optimal suas path planning in three-dimensional constrained environments. *Unmanned Systems*, 07(02):105-118.
https://doi.org/10.1142/S2301385019500031